17th Brazilian Congress of Thermal Sciences and Engineering
November 25th-28th, 2018, Águas de Lindóia, SP, Brazil

ENCIT-2018-0723
HEAT TRANSFER ANALYSIS OF A SUPERCRITICAL CARBON DIOXIDE NATURAL CIRCULATION LOOP

Gabriel Caetano Gomes Ribeiro da Silva
Jian Su
COPPE, Federal University of Rio de Janeiro - Nuclear Engineering Program
gcsilva@nuclear.ufrj.br ; sujian@nuclear.ufrj.br

Abstract. *Considering the advantages of employing supercritical fluids in the industry and the importance of passive cooling systems, specially in the nuclear sector, it is important to understand the thermalhydraulic behavior of a supercritical flow, whose properties vary sharply causing several implications in terms of project. A 3D stationary model was implemented in ANSYS Fluent to investigate the heat transfer deterioration threshold within a supercritical carbon dioxide natural circulation loop, as well as heat transfer performance based on relations between dimensionless numbers. The mass flow rate increased, as expected, with the heater power input increment until a maximum was reached and experienced a sudden decline afterwards, characterizing the beginning of the heat transfer deterioration regime. In addition, a correlation for Nusselt number as a function of Rayleigh was proposed for the system under regular heat transfer regime, that is before the advent of heat transfer deterioration regime.*

Keywords: *CFD, natural circulation, heat transfer deterioration, supercritical fluids, thermalhydraulics*

1. INTRODUCTION

Along with the establishment of sustainability goals within power generation sector, the development of new design concepts favoring efficiency and safety has been set in motion. The employment of supercritical thermodynamic cycles, for instance, holds several advantages such as higher efficiency, simplified design amongst others. In the nuclear sector, supercritical cooling remains on the experimental field although the Supercritical Water Reactor (SCWR) was chosen as one of the Generation IV advanced reactor models. For this purpose, further research on supercritical fluids thermalhydraulics and stability threshold is fundamental (Jain and Rizwan-uddin, 2008).

A natural circulation loop (NCL) is a physical model where heat is removed from a source, transported through adiabatic pipes and delivered to a sink exclusively by means of buoyancy, that is, without the use of any external machinery. The most common layout found in the literature is the rectangular NCL and there are, for this sytem, four basic configurations: (i) horizontal heater horizontal cooler (HHHC), (ii) horizontal heater vertical cooler (HHVC), (iii) vertical heater horizontal cooler and (iv) vertical heater vertical cooler (Archana *et al.*, 2015).

As it regards to nuclear passive safety requirements, the supercritical natural circulation loops (SCNCLs) comprise a new concept of core residual heat removal and can be an alternative to traditional subcritical loops in some cases, delivering higher flow rates and lower fluid temperature levels. Apart from the nuclear field, SCNCLs have other reported applications, such as solar thermosyphons, refrigeration systems and cooling of rotating machinery (Sarkar and Basu, 2017).

The variation of thermal physical properties in the vicinity of the pseudocritical point is very sharp and qualitatively similar for all fluids. Figure 1 shows the behavior of CO_2 at 9.0 MPa as stated by Zhang *et al.* (2010).

Supercritical natural circulation loops have been studied by a significant number of researchers both theoretical and experimentally. It has been reported by most authors that the main limitation of such systems is the appearance of the so called heat transfer deterioration phenomenon (HTD), which consists of a sudden fall in mass flow rate as a result of crossing a system inherent power threshold. This threshold corresponds to the point where the minimum temperature across the loop reaches the pseudocritical temperature. At this point, the density difference across the loop drops rapidly and so does the buoyancy. Consequently, friction forces start controlling the system, thus reducing the flow rate despite temperature difference between heater and cooler is kept high. Due to the lower coolant flow rate circulating in the loop, heat transfer coefficient declines and heater wall temperature increases rapidly (Sarkar and Basu, 2017).

An important remark is that, in literature, there are very few heat transfer correlations for natural circulation. The scarcity of correlations is, in part, due to the existence of several different behaviour zones, thus natural convection of an enclosed flow is considered a very complex phenomenon, although Yadav *et al.* (2012) have proposed a Nusselt correlation as a function of Reynolds number and Prandtl number for both subcritical and supercritical rectangular NCLs.

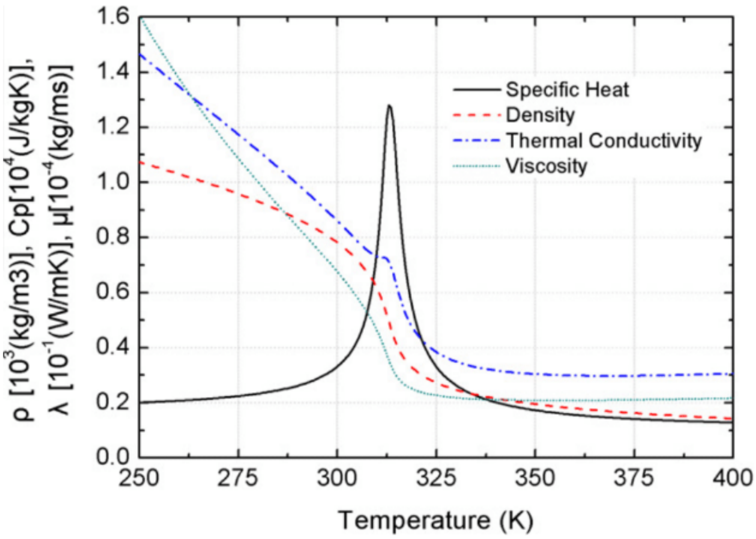

Figure 1. Variation of properties of CO_2 at 9.0 MPa

In order to model a rectangular SCNCL, certain features need to be accounted for. According to Archana *et al.* (2015), the two dimensional axis-symmetric model is only valid for the vertical heater and cooler configuration (VHVC) owing to the strong inherent asymmetry of the flow in horizontal heat exchangers. An extra particularity of this system is the high variation of density along the flow invalidating the use of Boussinesq approximation and, hence, the use of NIST real gas model is advised by most authors.

2. METHODOLOGY

Let us consider a rectangular natural circulation loop of height H and width W. The loop is perpendicular to the ground and the diameter of the tube (D) is uniform. The horizontal cooler and heater lie on the upper and lower portions of the loop, respectively, and their centers of mass are aligned with the center of mass of the loop. The cooler and heater have lengths L_C and L_H, respectively. The loop's geometry is depicted in Fig. 2.

A 3D steady state model was adopted. The boundary conditions are: (i) constant temperature T_C at the cooler, (ii) constant input power Q at the heater, (iii) adiabatic tubes.

The turbulence model utilized was RNG κ - ε and the governing equations are summarized hereinafter.

Conservation of mass equation:

$$\frac{\partial}{\partial x_j}\left(\rho u_j\right) = 0 \tag{1}$$

Conservation of momentum equation:

$$\frac{\partial}{\partial x_j}(\rho u_j u_i) = -\frac{\partial p}{\partial x_i} + \frac{\partial \tau_{ji}}{\partial x_j} + \rho g_i \tag{2}$$

The shear stress (τ_{ji}) is determined as follows:

$$\tau_{ji} = \mu_{eff}\left(\frac{\partial u_i}{\partial x_j} + \frac{\partial u_j}{\partial x_i} - \frac{2}{3}\delta_{ij}\frac{\partial u_j}{\partial x_j}\right) \tag{3}$$

The term μ_{eff} is the effective viscosity, or molecular viscosity, and is defined by:

$$\mu_{eff} = \mu + C_\mu \rho \frac{\kappa^2}{\varepsilon} \tag{4}$$

Here, C_μ is derived using RNG theory and equals to 0.0845, κ is the turbulent kinetic energy and ε is the turbulent dissipation rate.

The conservation of energy equation is:

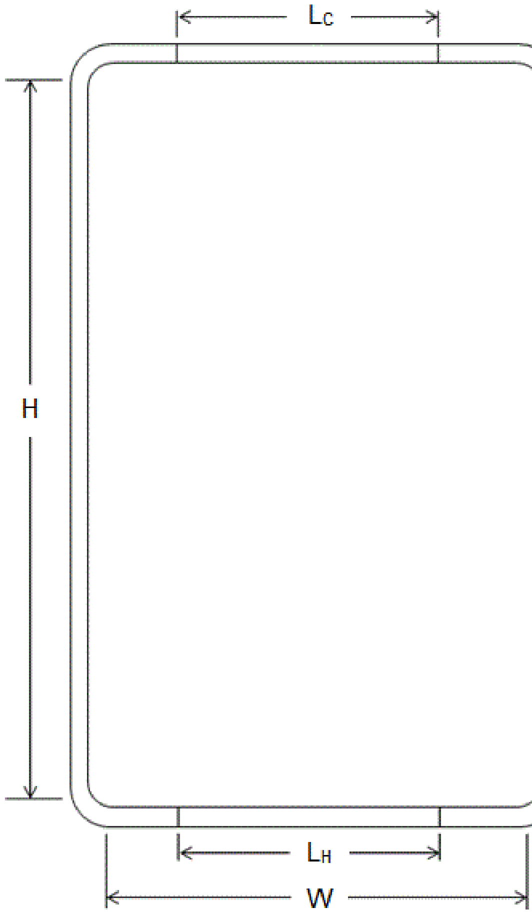

Figure 2. Geometry of the loop

$$\frac{\partial}{\partial x_j}(\rho u_j h_{tot}) = \frac{\partial}{\partial x_j}\left(k_{eff}\frac{\partial T}{\partial x_j} + u_j \tau_{ji}\right) \tag{5}$$

In the equation above, k_{eff} is the effective thermal conductivity and h_{tot}, the total enthalpy, determined by the following equation:

$$h_{tot} = h + \frac{1}{2}u_i^2 \tag{6}$$

The governing equations were solved numerically by using ANSYS Fluent v. 18.2, through the finite volume method. The discretization of the momentum equation was carried out with PRESTO and the other terms were discretized using second-order scheme. The pressure-velocity coupling was executed with the PISO algorithm.

In order to investigate the effect of buoyancy, turbulence and heat transfer, a series of dimensionless numbers have been used.

Reynolds number:

$$Re = \frac{D\dot{m}}{A\mu} \tag{7}$$

where $\dot{m}$ is the mas flow rate, A is the cross sectional area of the tube and μ is the fluid's viscosity.

Modified Grashof number:

$$Gr_m = \frac{gQ\beta D^3\rho^2 H}{A\mu^3 C_p} \tag{8}$$

where g stands for gravitational acceleration, Q is the thermal input of the heater, β is the volumetric expansion coefficient of the fluid, while ρ is its viscosity and C_p its heat capacity.

Nusselt number:

$$Nu = \frac{\bar{h}D}{k} \tag{9}$$

where $\bar{h}$ is the average heat transfer coefficient and k is the thermal conductivity of the fluid.

Prandtl number:

$$Pr = \frac{C_p \mu}{k} \tag{10}$$

Rayleigh Number:

$$Ra = Pr \cdot Gr \tag{11}$$

3. RESULTS AND DISCUSSION

For the simulation, the following parameters were considered: H = 800 mm, W = 600 mm, L_H = L_C = 400 mm, D = 8 mm. The tube wall was considered to be made of steel and have a 1 mm thickness. T_C = 298 K and the operating pressure was 8.5 MPa. Several steady state simulations were conducted for Q ranging from 50 to 850 W.

Four meshes were generated and mesh independence assessment was conducted comparing the steady state results for the simulation with the heater input of 330 W. Table 1 contains basic information of the meshes analyzed. Figure 3 shows the cross sections of the meshes in detail.

Table 1. Meshes indicators

Meshes	Number of elements	Number of nodes	Minimum orthogonal quality	Maximum skewness
1	23598	26496	0.839	0.396
2	106110	115280	0.856	0.396
3	185024	199892	0.862	0.403
4	268250	288600	0.862	0.411

The width of the first cell near the wall was kept the same for all meshes and corresponds to y^+ = 35, compatible with RNG κ - ε model with standard wall functions.

The results of the preliminary mesh independence analysis are presented in Fig. 4. It shows the values of cross sectional area averaged temperature along the length of the heater. In order to reduce computational time, the mesh 3 was chosen for the simulation.

For each steady state achieved along the power accession curve, the corresponding mass flow rate was observed. The outcome is shown in Fig. 5. It can be seen that the mass flow rate increases until it reaches a maximum and declines very rapidly beyond that point, as expected. It continues to fall eventually, but at a lower rate. This behaviour is an implication of heat transfer deterioration taking place in the system caused by the reduction of buoyancy force.

As it has been extensively discussed by several authors, it is possible to verify the validity of such simulation by comparing it with a Reynolds x modified Grashof number correlation. A correlation expressed by Swapnalee *et al.* (2012) is used for this purpose and the comparison is presented in Fig. 6. A good qualitative relationship can be observed although simulation values tend to be smaller than those predicted by the correlation. Such behavior is acceptable once the correlation is based on a experimental friction factor and averaged for all four existing loop configurations.

The temperature and velocity contours are portrayed in Fig. 7 over the heater midpoint cross section for both 500 W and 700 W of power. A strong asymmetry can be observed in all cases, which is expected for supercritical horizontal flows. The upper portion of the heater is hotter than the lower portion and that is due to the macroscopic movement caused by buoyancy and gravity acting over the same plane. This movement is shown by the vector field in the figure. The 700 W input contours, when compared to the 500 W case, show a bigger gradient of temperature and consequently, velocity over the cross sectional plane. This is caused by heat transfer deterioration leading to critical hotspots within the loop.

A graphic of Nusselt number against Rayleigh number is plotted in Fig. 8. It is evident that, for lower values of Ra, the relationship is more predictable once it is possible to draw a line on the log x log scale. This happens because, for lower values of Ra, part of the system still behaves as a single phase fluid and as Ra grows, the supercritical behaviour increases and the behaviour starts to change. After the beginning of HTD regime, the behaviour of the curve changes and

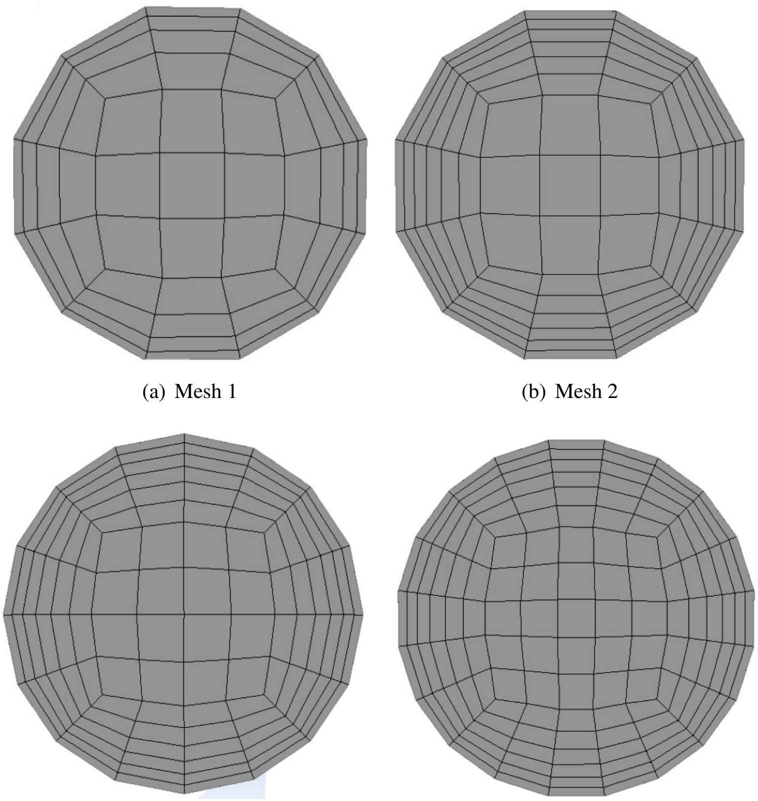

(a) Mesh 1 (b) Mesh 2

(c) Mesh 3 (d) Mesh 4

Figure 3. Cross sections of meshes

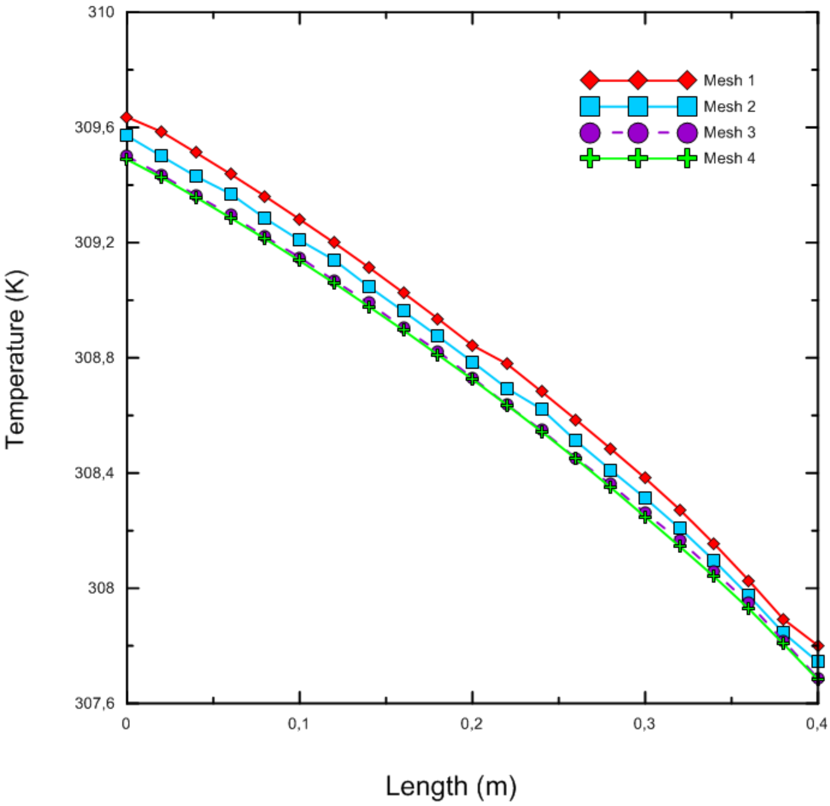

Figure 4. Mesh independence study of the temperature distribution along the heater

these points were left out from the graphic, thus, the proposed correlation is only valid for regular heat transfer regime. For a matter of comparison, two correlations were also plotted: Dittus-Boelter correlation, which is traditionally used to

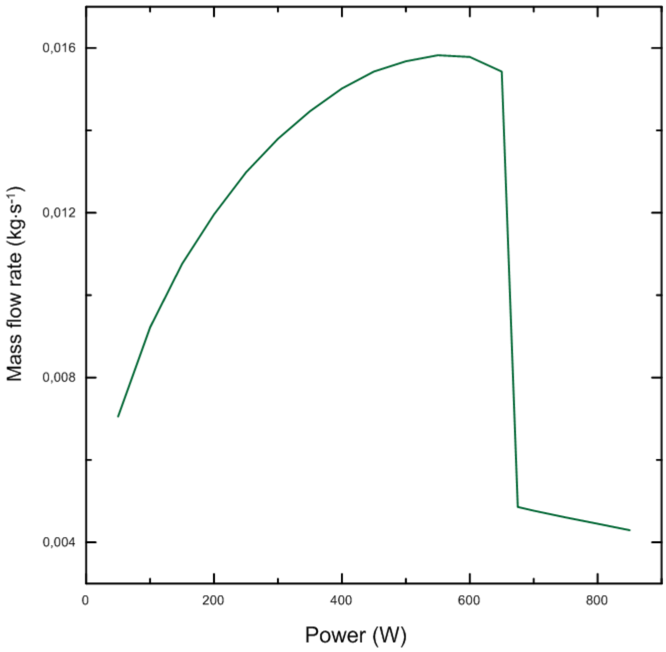

Figure 5. Mass flow rate as a function of heating power

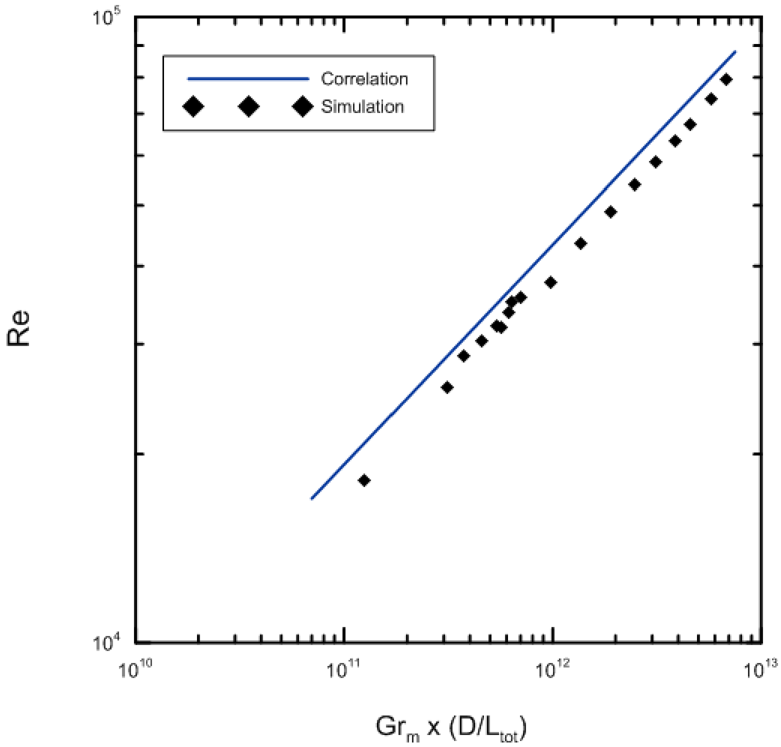

Figure 6. Reynolds number as a function of $Gr_m \times (D/L_{tot})$ in comparison with existing correlation from literature

estimate forced convection heat transfer, and the correlation from Yadav *et al.* (2012), which was developed for natural circulation. The Dittus-Boelter correlation presents great discrepancy, as expected, and the correlation from Yadav *et al.* (2012) presents a good agreement, specially near heat transfer peak, which is characterized by the highest Nusselt number and the highest mass flow rate.

The proposed correlation is the following:

$$Nu = 9.53 \times 10^{-3} \cdot Ra^{0.293} \tag{12}$$

The corresponding average Prandtl number is 5.56 and it is expected to provide good estimation of heat transfer coefficient for similar range of parameters and it is not expected to be valid for heat deterioration regime.

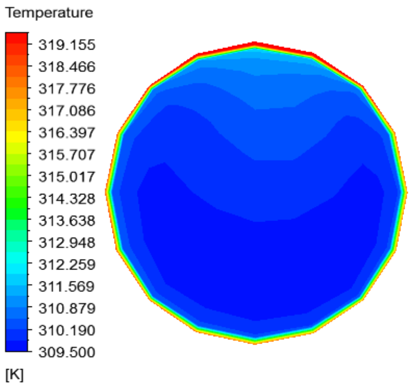

(a) Temperature at 500 W

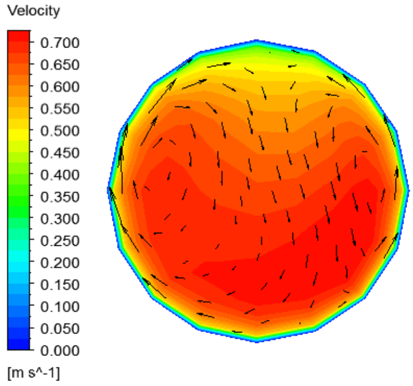

(b) Velocity at 500 W

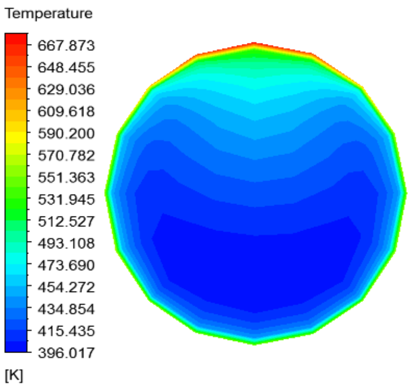

(c) Temperature at 700 W

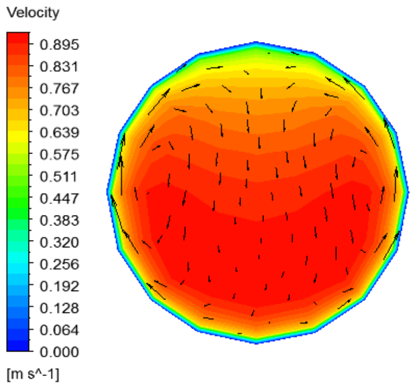

(d) Velocity at 700 W

Figure 7. Temperature and velocity contours on heater midpoint cross section

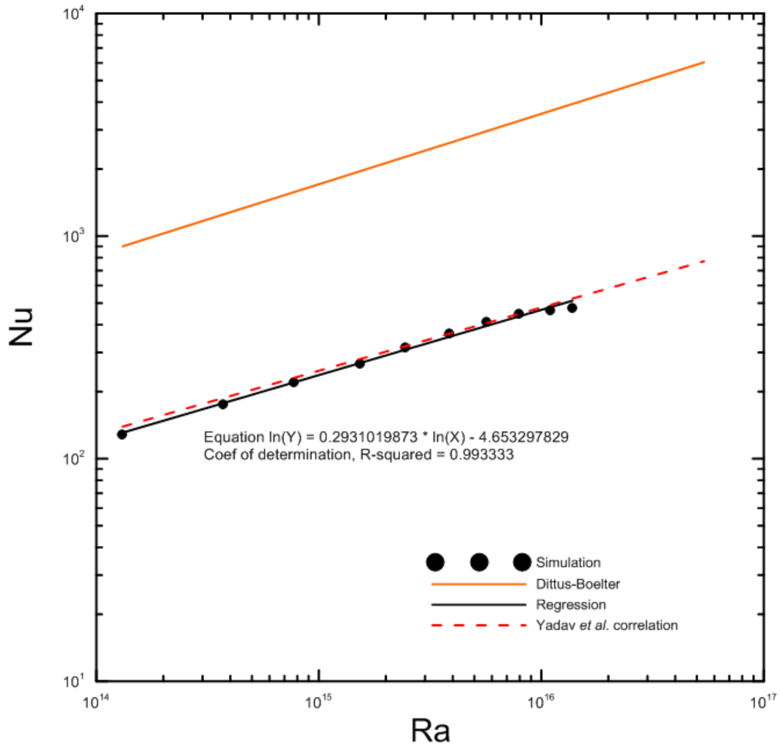

Figure 8. Relation between Nu and Ra for heat transfer before the advent of HTD

4. CONCLUSIONS

The present geometry is able to operate in steady state for a specific range of parameters and the power increment causes the mass flow rate to rise until it reaches a maximum. After this value, the HTD regime takes over. Strong asymmetry can be observed in the system due to high local buoyancy caused by the sharp variation of properties near the pseudocritical point, thus, the 3D model is indeed the most appropriate for this system. Even for low Rayleigh numbers, the Dittus-Boelter correlation does not provide a good heat transfer estimate, whereas, the correlation from Yadav *et al.* (2012) provides a good estimate, specially near the heat transfer peak. Considering the lack of heat transfer correlations for natural circulation loops, computational fluid dynamics may be an effective tool to help covering such gap and contribute to passive security system projects. The proposed correlation may provide a good heat transfer estimate for supercritical natural circulation loops operating under regular heat transfer regime for Prandtl numbers close to the one in this study.

5. REFERENCES

Archana, V., Vaidya, A. and Vijayan, P., 2015. "Numerical modeling of supercritical CO2 natural circulation loop". *Nuclear Engineering and Design*, Vol. 293, pp. 330–345.

Jain, P.K. and Rizwan-uddin, 2008. "Numerical analysis of supercritical flow instabilities in a natural circulation loop". *Nuclear Engineering and Design*, Vol. 238, No. 8, pp. 1947–1957.

Sarkar, M.K.S. and Basu, D.N., 2017. "Numerical Comparison of Thermalhydraulic Aspects of Supercritical Carbon Dioxide and Subcritical Water-Based Natural Circulation Loop". *Nuclear Engineering and Technology*, Vol. 49, No. 1, pp. 103–112.

Swapnalee, B., Vijayan, P., Sharma, M. and Pilkhwal, D., 2012. "Steady state flow and static instability of supercritical natural circulation loops". *Nuclear Engineering and Design*, Vol. 245, pp. 99–112.

Yadav, A.K., Ram Gopal, M. and Bhattacharyya, S., 2012. "CO2 based natural circulation loops: New correlations for friction and heat transfer". *International Journal of Heat and Mass Transfer*, Vol. 55, No. 17-18, pp. 4621–4630.

Zhang, X.R., Chen, L. and Yamaguchi, H., 2010. "Natural convective flow and heat transfer of supercritical CO2 in a rectangular circulation loop". *International Journal of Heat and Mass Transfer*, Vol. 53, No. 19-20, pp. 4112–4122.

6. RESPONSIBILITY NOTICE

The authors are the only responsible for the printed material included in this paper.